

Analysis of MoFrac-Generated Deterministic and Stochastic Discrete Fracture Network Models

Junkin, W.R. and Fava, L.

MIRARCO Mining Innovation, Sudbury, ON, Canada

Laurentian University, Sudbury, ON, Canada

Ben-Awuah, E.

Laurentian University, Sudbury, ON, Canada

Srivastava, R.M.

FSS Consultants, Toronto, ON, Canada

Copyright 2018 ARMA, American Rock Mechanics Association

This paper was prepared for presentation at the 2nd International Discrete Fracture Network Engineering Conference held in Seattle, Washington, USA, 20–22 June 2018. This paper was selected for presentation at the symposium by an ARMA Technical Program Committee based on a technical and critical review of the paper by a minimum of two technical reviewers. The material, as presented, does not necessarily reflect any position of ARMA, its officers, or members. Electronic reproduction, distribution, or storage of any part of this paper for commercial purposes without the written consent of ARMA is prohibited. Permission to reproduce in print is restricted to an abstract of not more than 200 words; illustrations may not be copied. The abstract must contain conspicuous acknowledgement of where and by whom the paper was presented.

ABSTRACT: MoFrac discrete fracture network (DFN) modeling software generates fracture network simulations with deterministic fractures constrained to known locations, and stochastic fractures conditioned to input data. A deterministic fracture network is generated through the modeling of a dataset that is representative of the lineaments typically found in a Canadian Shield environment. This model is used to constrain stochastic representations to observed fracture intensities and orientations. This study considers two-dimensional and three-dimensional length distributions and area distributions as constraints. Built-in metrics are used to analyze the size and orientation distributions of the stochastic models for comparison with the input data. Further calibration of constraints for these models is achieved by dividing fracture groups into subsets; this preprocessing task involves the definition of subsets of identified fracture groups based on orientation. The consistency and accuracy of the fracture network modeling are considered using three alternative conditioning methods. It was shown that generated fracture networks conform to the conditioning parameters for each method considered. Where multiple subsets were used to define fracture group parameters, resulting DFNs were more representative of the input data.

1. OVERVIEW

A discrete fracture network (DFN) maps the location of discontinuities within a rockmass. MoFrac DFN modeling software has been developed based on the methodologies of FXSIM3D (Srivastava, 2006). Using MoFrac, a *deterministic* fracture can be modeled using data from a mapped trace and a *stochastic* fracture can be created using attributes conditioned to known data. A hybrid model of a DFN includes both types of fractures. Stochastic fractures infill where data is not reliable or where mapping has not occurred within a model domain. This study examines the conditioning and consistency of stochastic fractures generated by MoFrac.

From a fracture trace mapped on a surface, the propagation of a deterministic fracture is guided by conditioning variables such as orientation, strike to dip ratio, and size. All realizations of deterministic fractures intersect traces on the mapped surface, however the realizations diverge according to the variance specified by assigned input variables. In MoFrac, stochastic fractures can be generated using three alternative methods related to the definition of fracture intensity and size.

A cumulative length distribution (CLD) can be measured directly from an input dataset and used as an input for

conditioning stochastic fractures to observed intensities. The CLD approach works well when all fractures are seeded from a single plane; for example, a surface study where no fractures are seeded at depth. When considering a rockmass volume, and in order to use CLD values measured on a surface, fracture intensities must be modified to reflect the depth of the model. This approach generates a model constrained by a three-dimensional length distribution.

Alternatively, a cumulative area distribution (CAD) can be used as an input for defining stochastic fracture intensity. This method is suited for seeding fractures within a volume of rock, however measuring this value *in situ* is difficult. The surface area of a fracture is generally unknown and must be derived either through preprocessing or by analysis of a simple DFN generated from the mapped data (Dershowitz and Herda, 1992; Niven and Deutsch, 2010; Lei, *et al.*, 2017).

This study considers both types of size distributions to define stochastic fracture intensities constrained to an input dataset. The consistency of the DFN models generated and the degree of constraint is examined. Fracture orientations, sizes, and intensities are compared for multiple realizations of DFNs. The derivation of CLD and CAD values are presented and the MoFrac-generated DFNs are analyzed to confirm realization of input

variables. A dataset designed to be representative of the Canadian Shield is used to generate a deterministic DFN and to constrain the stochastic networks that are subsequently generated.

2. CANADIAN SHIELD DATASET

The dataset used to model deterministic fractures was developed to be a realistic approximation of the expression of fractures on surface in a setting typical of the Canadian Shield. This dataset was developed for the Third Case Study of the deep geological repository technical program of Ontario Power Generation (Gierszewski, *et al.*, 2004). The Third Case Study dataset was derived from a group of surface lineaments interpreted from an aerial photograph shown in Figure 1; additionally, simulated fracture traces are incorporated into the network to match fracture intensities recorded at a separate and representative location (Srivastava, 2002). The final dataset, shown in Figure 2, covers approximately 200 km² of land that is representative of a typical section of the Canadian Shield.

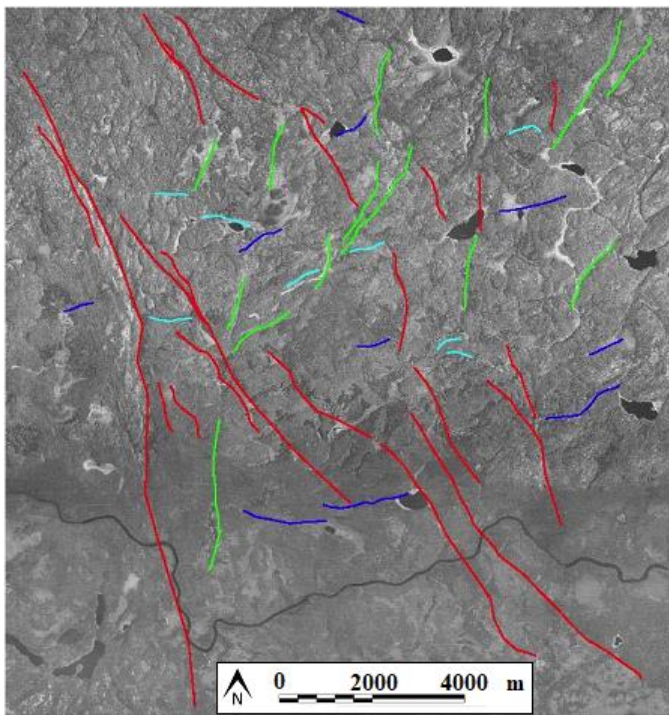


Fig. 1. Automatically detected surface lineaments superimposed on a composite aerial photograph; used to generate the Canadian Shield dataset (Srivastava, 2002)

3. MOFRAC SOFTWARE

MoFrac DFN modeling software generates a fracture as an approximately equilateral, tessellated triangular mesh. A deterministic fracture is propagated from a surface lineament guided by values for orientation, size, and shape sampled from distributions derived from the input data. Stochastic fractures seeded using a length

distribution originate from a simulated trace and are propagated in an analogous method to deterministic fractures. When using an area distribution, stochastic fractures are seeded from a single point and propagate concentrically to form a tessellated mesh. Junkin *et al.* (2017) described, in further detail, the fracture propagation process of the MoFrac software.

Measured orientations are assigned to a mapped fracture trace; for this study the strike is measured from the data as the direction of a straight line segment between terminal points of a trace and dip angles are set to 90° for all fractures.

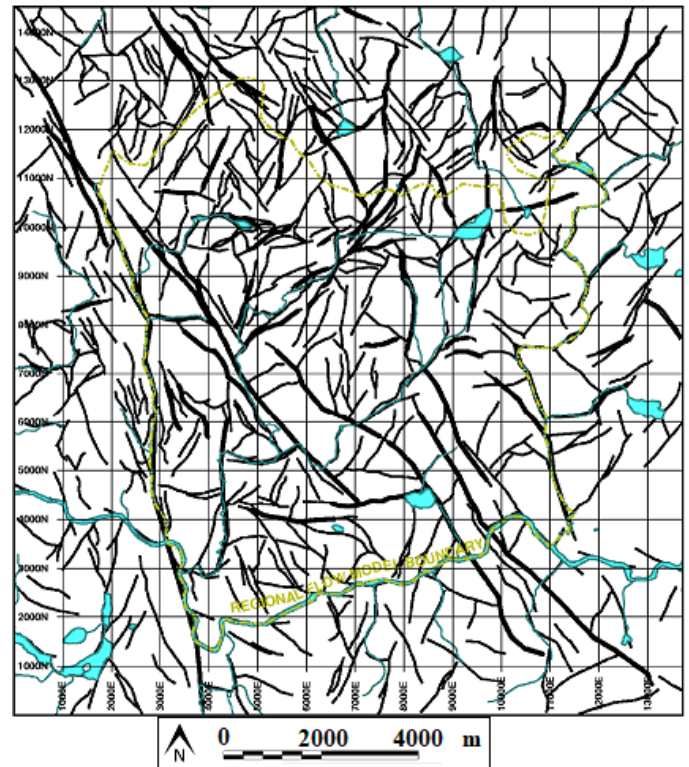


Fig. 2. Integrated Canadian Shield dataset including simulated fractures shown with surficial water features (Srivastava, 2002)

Stochastic fractures are seeded in one of three ways. When using the CAD intensity input, a fracture is seeded randomly within the volume and is assigned a target surface area and orientation. The fracture propagates concentrically from a central point until the assigned surface area is reached. When using the CLD intensity input, a fracture is seeded randomly on a horizontal plane, and the assigned size governs the length of the seed trace. The fracture then propagates using the same process as for deterministic fractures. When it is desired to have fractures seeded at random depths in a three dimensional domain, the CLD intensity input can be used where the z value is randomized. For this case, input intensities are multiplied by a factor related to the model depth as a function of mean trace length. The increased intensity is distributed throughout the model domain with the goal of

any measured plane having P_{21} values constrained to the mapped data.

4. DFN PARAMETERS

Four sets of DFN models are analyzed in this study - fifty realizations each of: (i) deterministic models based entirely on the Canadian Shield dataset, (ii) stochastic models with intensities derived from the measured CLD and seeded entirely on surface, (iii) models with intensities derived from the CLD and seeded throughout the domain, called the CLDz model, and (iv) models with intensities derived from the CAD that are seeded throughout the domain.

4.1 Fracture Orientation

Only the spatial locations of the fracture traces were used as an initial input for DFN modeling. To determine fracture orientations, a preliminary deterministic model was generated with four fracture groups (strikes of 0° , 90° , 180° , and 270°). The results of this model are shown in Figure 3 with a Wulff stereonet of the orientations created using Dips version 6 (Rocscience, 2016). Two fracture groups were identified on this stereonet and the strikes were interpreted to be 298° and 240° .

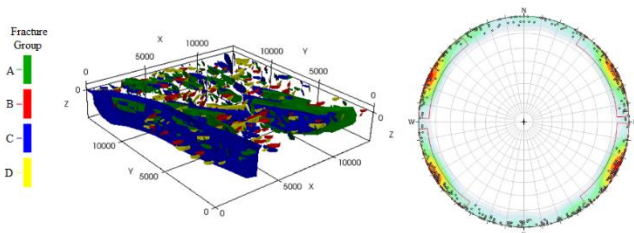


Fig. 3. Preliminary DFN model based on the Third Case Study dataset with Wulff stereonet showing measured dip directions.

4.2 Fracture Intensity and Size Distributions

The Third Case Study dataset consists of 553 fracture traces ranging in size from 68 to 15,000 m. Two orientation groups were identified through the preliminary modeling. Group 1 consisted of 272 fractures with a strike of 298° ; group 2 consisted of 281 fractures with a strike of 240° . The calculated CLD curve is shown in Figure 4. The surface area of modeled fractures was determined based on the initial deterministic DFN. Surface areas ranged from 2,000 to 45,000,000 m^2 . As the input data only gives fractures that intersect with the surface, two CAD curves are presented. The CAD2k curve considers the entire model to a depth of 2000 m and the CAD68 curve considers only the uppermost 68 meters of the volume. This sample of the model domain ensures that every fracture is represented along any horizontal plane. The input intensity when considering CAD distributions should thus be between these two distributions. The calculated CAD curves are shown in Figure 5.

Input intensities for DFN modeling were derived from the measured intensity curves. For fracture intensities derived from the CLD curve, a multiplier must be used if it is desired to have fractures seeded throughout the experimental volume (Junkin *et al.*, 2017). The factor used as a starting point for converting fracture intensities from a CLD curve to an input related to an experimental volume (CLDz) is derived by considering the model depth and the mean trace length for each identified group.

$$CLDz = CLD \times \left(\frac{\text{model height}}{\text{mean trace length}} \right) \quad (1)$$

The multiplier is applied to both ends of the CLD input curve; the initial curve is fit to the power law regression line of the measured CLD curve. The power law has been shown to be a representative approximation of measured intensity distributions for fracture networks (Bonnet *et al.*, 2001; Neuman, 2008). The derived input intensity for the minimum size of fracture is the intersection of the power law regression line to the data, and the intensity for the maximum size is the point on the same regression line that matches the largest measured fracture. The input values for the CLD models and for the CLDz models, where the factor shown in Equation 1 is used, are shown in Figure 4.

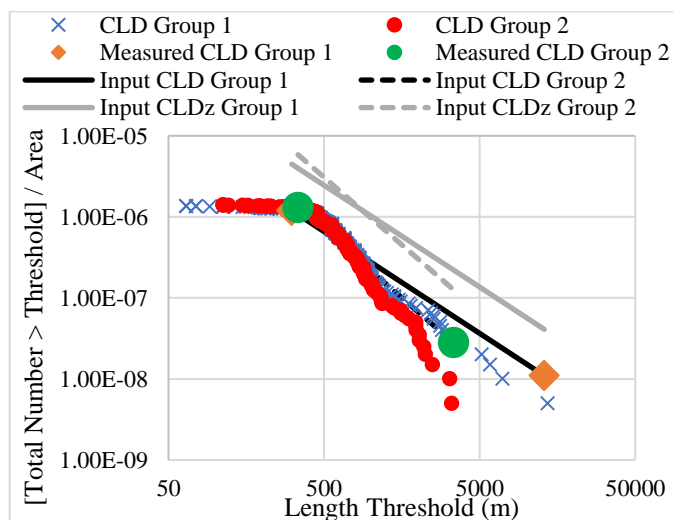


Fig. 4. CLD and CLDz input intensities for stochastic models as derived from measured CLD curve from preliminary model.

For the DFN models generated with intensities from a CAD function, input values were derived from distributions describing the deterministic data set throughout the whole volume (CAD2k). To derive input intensities from the CAD, the surface area values used as nodes on the CAD curve were doubled to account for modeling elliptical fractures (as opposed to semicircular in the preliminary runs where fracture surface area was initially measured). The intensity value was also modified by a factor equivalent to that used for the CLDz model in order to account for the size of the fracture related to the volume in which the CAD was measured. The CAD multiplier used is given by Equation 2.

$$CAD_{input} = CAD \times \left(\frac{\text{model height}}{2 \times \sqrt{\text{mean fracture area}/\pi}} \right) \quad (2)$$

The final intensities used for stochastic modeling based on the CAD distribution for the Canadian Shield dataset are shown in Figure 5. Table 1 summarizes the benefits and consequences of the three methods used to constrain fracture size and intensity; a brief description of the seeding process is included.

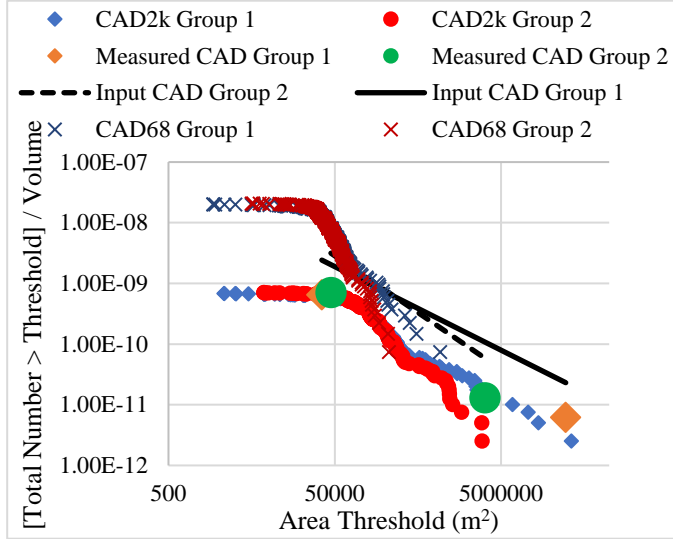


Fig. 5. CAD input intensities for stochastic models as derived from measured CAD curve from preliminary model.

4.3 Additional DFN Parameters

Fracture orientation and intensity are conditioned to deterministic data; however, additional DFN parameters are required for modeling. The undulation of fractures is controlled through a parameter that is selected by visually matching fractures in the dataset to stochastic fractures with the same waviness. This parameter can be derived by measuring the sinuosity of a fracture group. The undulation parameter was derived for each group and was kept constant between all models described in this study, as were other geometric variables including truncation probabilities, strike to dip ratio, TAC (terminal area constraint) factor, scaling and shape. The values used for these parameters are given in Table 2. The strike to dip ratio determines the geometry of the guiding shape for the fracture, and the TAC factor determines the location of the mapped trace on the guiding shape. A strike to dip ratio of 1 and TAC factor of 1 results in circular disc shaped fractures with the fracture trace as the central chord. Fractures with these parameters are modeled as semi-circles when traces are located on a boundary of the model as in a surface study.

Fifty DFN models were generated for each of the four types of models described. All blocks have the same dimensions, $13,725 \times 14,550 \text{ m}^2$, matching the

deterministic dataset. The models are extended to a depth of 2,500 m.

5. ANALYSIS OF DFN MODELS

Fifty realizations of each of the four types of models were generated. Orientations, intensities and fracture size were analyzed, with consideration of variance between the fifty realizations. The observed output was compared directly to the input parameters used for modeling. The results from each type of model will be presented in the four subsections that follow. Figure 6 considers, for a randomly selected realization, the CLD and CLDz inputs for stochastic models in comparison with the actual intensities by group. For the CLDz models, input intensity is a measure of the intensity derived from the lengths of all fracture traces within the model projected onto the surface. Figure 7 considers the CAD input for stochastic models and actual intensities from another randomly selected realization.

The orientations for all fifty realizations consistently matched the input orientations. Cumulative Wulff stereonets are presented in Figure 8 for each of the four types of models considered. It should be noted that, for strikes of 0° and 180° , there is an under-representation of fractures in the stochastic models, as only two fracture groups were used. In order to create the same clustering of fractures around the two dominant orientations and have representation of the fractures with random orientations included in the model, additional fracture groups are required.

Figure 9 shows single realizations of each model type with inspection planes taken at surface and at -500 m. The inspection plane at depth is used to demonstrate the usefulness of a DFN model based on surface mapping for predicting fracture intensities at depths relevant to the workings of an underground mine or a deep geological repository. P_{32} values of the whole models are considered as well as P_{21} values for each of the inspection planes. These measures are independent of scale and useful as metrics to consider the constraints applied to the DFN models (Dershowitz and Herda, 1992).

5.1 Deterministic Models

Fifty realizations of a deterministic model were generated in addition to the stochastic models. The orientation of fractures that is reported by MoFrac as measured on surface is consistent between realizations.

The consistency in orientations between deterministic models is due to the constraints of surface traces for all fractures. The ability of MoFrac to match a trace location is assessed through a built-in metric that considers the longitudinal root mean squared error (LRMSE) between the input trace and the trace representing the modeled fracture on the same surface (Anderson and Ames, 2013).

Fractures were consistently modeled with location errors ranging between approximately 2 and 300 m. Five of the eight largest fractures had the largest location errors. The location error showed a scale dependency, with the highest 25 location errors measured from fractures in the first 100 when considering trace length. A mean location error of 14.4 m was calculated for the fifty realizations, with a standard deviation of 27.3 m.

Table 1. Methods used to constrain fracture size and intensity to DFN models representing the Canadian Shield dataset.

DFN Model	Fracture Seeding	Benefit	Consequence
CAD	Fractures are seeded at a random point, propagating concentrically	Fractures are not constrained by an arbitrary trace Interactions between boundaries and simulated traces do not occur	Size distributions must be derived that apply to a volume Seed points close to boundaries can result in malformed fractures
CLD	Fractures are seeded from a simulated lineament on the $z = 0$ plane	Fracture intensities are applied in the same dimension that they are measured A DFN model similar to mapped data is generated	Fractures are only modeled as seeded on a single plane within a model No fractures are seeded at depth, as such intensities drop considerably with depth
CLDz	Fractures are seeded from a simulated trace on any plane within the model	Applied fracture intensities are modified directly from mapped data Fracture intensities are consistent regardless of depth	Fractures can be seeded at any depth but traces are always orientated horizontally Simulated traces are treated as deterministic traces

Table 2. DFN modeling parameters that are consistent between all models.

DFN parameter	Value
Probability of truncation	1 between subgroups and regions 0 between groups
Strike to dip ratio	1 (preliminary runs) 0.25-4 (final runs)
TAC factor	1 (preliminary runs) 1-4 (final runs)
Scaling	16-32 elements per fracture (preliminary runs) 1000-2000 elements per fracture (final runs)
Shape	All fractures are elliptical
Undulation	Group 1 sinuosity 1.029 Group 2 sinuosity 1.025

The intensities measured in Figure 9 demonstrate that, when only deterministic fractures are included in a model, a drastic decrease in intensity is observed at depth in all realizations. This is shown both by P_{32} values for the entire models and by comparing P_{21} values at surface and a depth of 500 m for each model type. This is expected, as fractures are only seeded on the surface of the CLD model with fracture intensities constrained to mapped intensities. Borehole data, if available, can constrain intensities with depth.

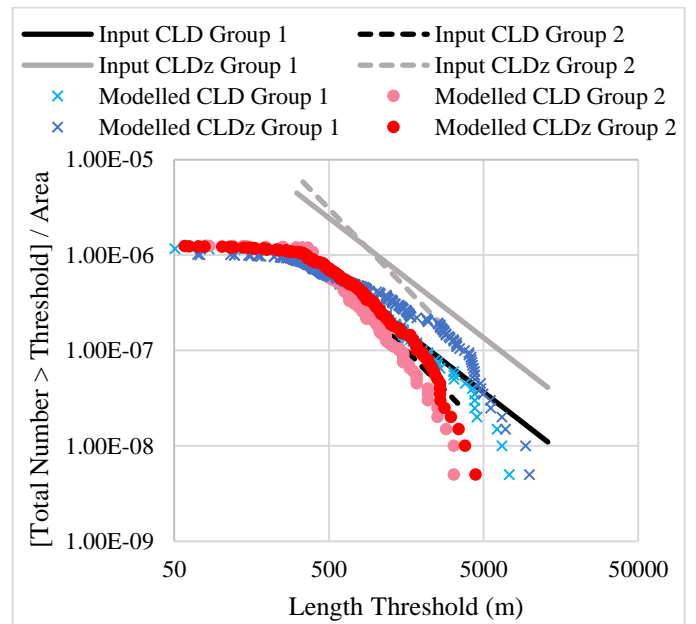


Fig. 6. Input intensities for stochastic models derived from the measured CLD with actual CLD curve measured from representative models.

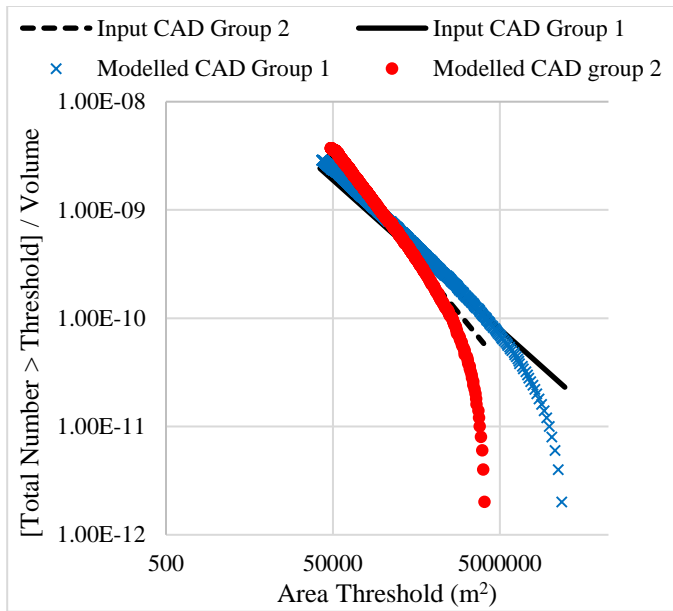


Fig. 7. Input intensities for the stochastic model derived from the measured CAD with measured curve from a representative model.

5.2 Stochastic DFN models

Fifty realizations of each of the three types of stochastic models were generated for analysis. The location of each fracture is randomized, so a location metric is not applicable. The orientations of fractures generated were shown to be consistent between all realizations. Although the calculated fracture groups are consistent, there is a difference noted in the ratio between the numbers of fractures in each group. This effect is exacerbated in the models that consider fractures seeded throughout the model, demonstrating that it is a cumulative effect. Consideration should be given to this effect when fracture groups with large ranges in size are modeled together using MoFrac. The variance in intensities between all realizations of stochastic models are shown in Figure 10; these are compared with the variance in intensities between the deterministic realizations. The variation in P_{21} values at surface and at a depth of -500 m are considered for all models generated.

5.3 Two Dimensional Length Distribution Model (CLD)

Fractures are only seeded on surface in the CLD model; this matches the deterministic data in terms of the planar location of fracture centroids. As no fractures are seeded at depth, the decrease in intensity with depth observed in the deterministic models is also observed in the stochastic models. With a strike to dip ratio randomized from 0.25 - 4 and a TAC factor randomized from 1 - 4, there is variance between the models. This variation was used for all deterministic and stochastic models.

The observed decrease in intensity with depth is unavoidable and matches the deterministic data. Intensity levels thus match the deterministic model on surface and

at depth, as shown in Figure 9. This is useful when stochastically filling areas adjacent to a mapped block, in order to mimic the limitations of mapping occurring only on surface. Fracture intensities and size are considered in Figure 6. No fractures are generated with a size greater than the maximum value for the CLD input. There are fractures with lengths of 50 m—shorter than the minimum input length of approximately 300 m. The inclusion of fractures with lengths shorter than the minimum input value is due to the truncation of fractures. These truncated fractures result in a CLD curve that is very similar to the measured curve used as a constraint.

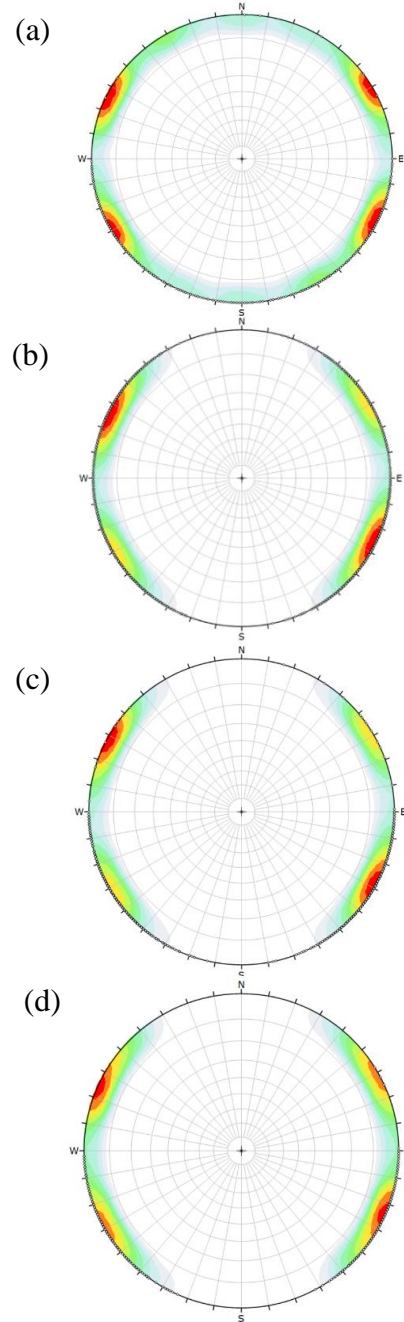


Fig. 8. Cumulative Wulff stereonet showing fracture pole densities for (a) deterministic models, (b) CAD stochastic models, (c) CLDz stochastic models, and (d) CLD stochastic models.

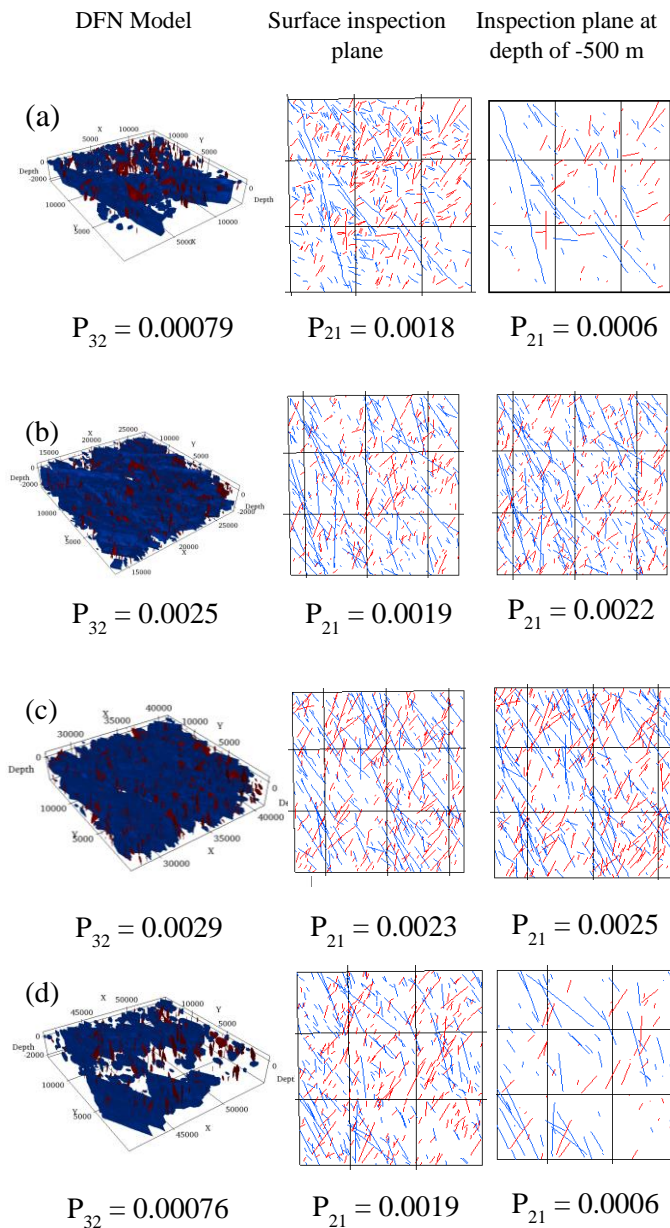


Fig. 9. DFN with measured P_{32} values and inspection planes with measured P_{21} values at $z = 0$ and $z = -500$ for (a) deterministic model, (b) CAD stochastic model, (c) CLDz stochastic model, and (d) CLD stochastic model.

5.4 Three Dimensional Length Distribution Model (CLDz)

The CLDz models use a modified CLD input with a randomized depth value that falls within the model domain. The observed orientations are consistent between all models, and the inclusion of fractures with lengths less than the input threshold is also observed. Comparing the curves from inspection planes on surface, shown in Figure 6, it can be seen that the CLDz curve shows a higher proportion of larger fractures in the midrange of the distribution. The ultimate length is constrained to the maximum CLD value, although fractures with a slightly longer trace length on surface are observed. The increased intensities in the midrange of the distribution can be

attributed to large fractures that are seeded at depth that propagate to the inspected surface. These fractures are not limited to a partial ellipse as are fractures seeded on surface that are truncated against the $z = 0$ boundary. This effect also contributes to the increased intensities observed for both stochastic models with seeding throughout the volume. The distance a fracture propagates from a trace is limited by the strike to dip ratio and TAC factor, and these input values should be considered when deriving intensities to fill a volume.

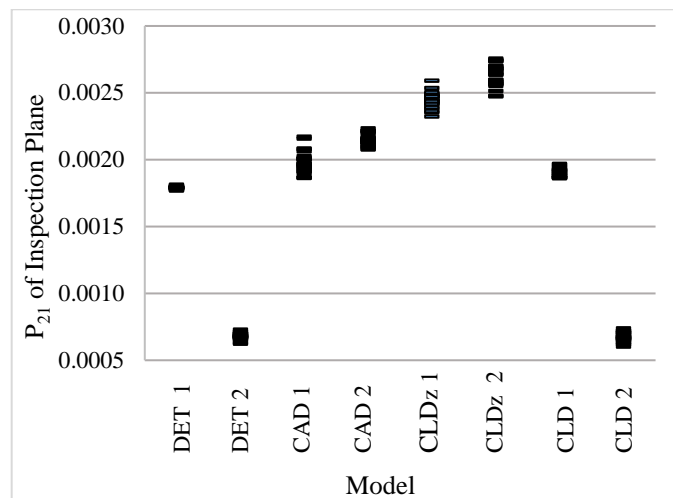


Fig. 10. Variance of intensities for deterministic and stochastic models at $z = 0$ (denoted as 1) and $z = 500$ (denoted as 2).

5.5 Area Distribution Model (CAD)

Although the CAD values were measured from the preliminary DFN, the input values required modification to account for the fact that all of the fractures were mapped on a single surface. Any fractures that exist in the rockmass that do not intersect the surface are not included, so there is an expected intensity decrease as the measured volume is increased. To account for this, a factor analogous to that used to generate the CLDz values was applied to the measured CAD values. The generated CAD and CLDz models are very similar and show the same characteristic increase in intensity, as fractures that are seeded at depth can propagate to a full ellipse, unlike surface fractures. Figure 7 considers a measured CAD curve in comparison to input values. It should be noted that, when using the CAD function for intensity input, fractures are seeded according to their sampled size. This means that fractures are not truncated on regional boundaries. This results in no fracture sizes less than the minimum input used as a constraint. Although the input is honored, the resulting CAD curve is different from the deterministic CAD curve, as fractures shorter than the minimum threshold are not included. Orientations are again consistent between models, with the same change in the ratio of fractures in groups as observed with the CLDz models. The under-representation of fractures with random orientations is also observed, and can be remedied by including additional fracture groups. There

is an identifiable similarity between the effects of the factor used to modify input intensities for both CLD and CAD inputs. This factor is reasonable and approximates required intensities for DFN modeling based on mapped surfaces. Further study into the dimensional independence of this factor is warranted.

5.6 Improving constraints with additional preprocessing

In order to account for some of the discrepancies observed between the deterministic models and the stochastic representations in this study, a supplementary DFN model was generated. This model was constrained with an additional fracture group to represent the random fractures observed in the Canadian Shield dataset. Two subgroups were also identified for each defined fracture group, based on size. This allows for differences in orientation and slope of the intensity input relative to fracture size. The purpose of this process is to generate a DFN model that is constrained to the deterministic data to a higher degree. A CLDz model was chosen for this process, as smaller fractures than the minimum size threshold are included in the model, resulting in a closer approximation to intensities observed in the input dataset. The resulting DFN model is shown in Figure 11. The random group is assigned a strike of 8° and the fracture groups from the previous model with strikes of 298° and 240° are retained for the modeling. Revised fracture intensity inputs are shown in Figure 12, with the measured values from the DFN model for comparison. The factor given in Equation 1 is applied separately to both the small and large fractures. This results in a distinct slope for each subgroup. The deterministic intensities used to define the constraints are included in Figure 12 for comparison. Note that the input intensities for the CLDz model are higher than the observed intensities on a plane. The difference between these intensities is a function of model depth. This is demonstrated in Figure 6 where input intensities are calculated for both CLD and CLDz models from a mapped surface.

Fractures with a trace length less than the minimum threshold are again observed, and measured intensities are constrained to the inputs. The effect of an increased density due to fractures propagating to the area of the guiding shape is reduced slightly. This is demonstrated by the CLD curve in Figure 12 and measured P_{21} values at surface and depth in Figure 11.

The resulting stereonet from the improved DFN model is shown in Figure 13. The additional preprocessing and definition of a random fracture group results in a stereonet that better approximates the measured orientations. The ratio of fractures between the two main fracture groups is well constrained with the addition of the third fracture group. The under-representation of random fractures is still evident but to a lesser degree. The difference in slope for the CLD for small and large fractures of each group

results in a measured distribution that modifies the generalized power law relation for a single fracture group.

6. DISCUSSION

For all fifty realizations, deterministic models were consistently constrained by the location of the input traces. A low variance in intensities at surface and depth was observed between the realizations.

Orientations were constrained by the fracture traces. Analyzing the reported LRMSE values for all deterministic runs, the fracture demonstrating the worst fit was consistently fracture 8. The tessellation of the fracture surface during propagation and the guiding shape contribute to slight changes in LRMSE values between models. As a fracture propagates, elements at depth must be connected to elements that are constrained at surface and, to maintain the integrity of the meshed surface during this process, variations in the fracture's trace at surface are observed. Figure 14 shows the input trace for fracture 8 with ten realizations from deterministic models. The realizations, when superimposed, demonstrate similarity regardless of differences in calculated LRSME values. Because fracture 8 demonstrates an unusual geometry in that the direction changes by almost 360° , MoFrac is unable to fit a suitable guiding shape to the trace that would allow for a match with the generated fracture. In cases such as this, fractures must be dealt with on an individual basis. For fracture 8, it would be sufficient to break the trace into two components and model them separately in order to have an accurate representation at depth.

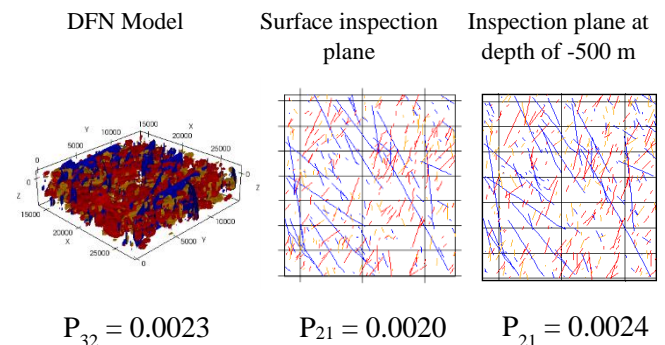


Fig. 11. DFN model generated with parameters derived from additional preprocessing.

The three stochastic models showed consistency between realizations, and are limited by the amount of preprocessing before modeling. When comparing the results of the three methods to constrain size and intensity, two major differences between models are identified.

When using a CLD input that is not modified from the measured values, a DFN is generated that matches mapped data accurately. The decrease in intensity with

depth is reproduced, as fractures are only seeded on the surface of the model. If it is desired to match mapped data as accurately as possible, this method is sufficient. Intensity constraints are simple to calculate and are reflected throughout the volume.

Where it is desired to have intensities at depth that are representative of mapped data on a surface and are consistent, it is necessary to seed fractures throughout the volume. This can be achieved using the CLDz or CAD intensity input. When using a CLDz input, fractures smaller than the minimum threshold are included in the resulting model due to truncations at boundaries. This is useful when constraining stochastic intensities to mapped fractures using a power law regression line. Smaller fractures can often be under-represented due to mapping bias, and the measured intensities are often less than a power law regression line would suggest. The mapping bias associated with larger fractures in relation to the size of the mapped domain is reproduced with the CLDz and CAD models as a function of the input intensity for the largest fractures.

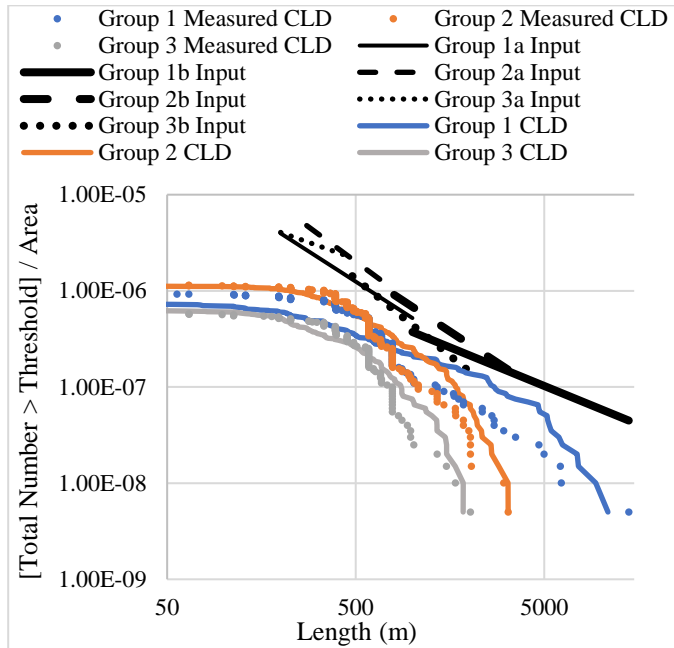


Fig. 12. Measured intensity on surface of DFN model generated with parameters derived from additional preprocessing in comparison to measured deterministic intensities.

It is shown that additional preprocessing of data allows for a more constrained DFN model. This is useful when it is desired to match input data as accurately as possible. If mapped data is used to simply guide the constraints, it is shown that constrained DFN models can be generated consistently. When constraining stochastic DFN models to mapped data from a single plane, such as with surface mapping, using the CLDz approach is recommended with MoFrac. This is because intensity values are derived directly from the input data and smaller fractures than the

minimum threshold are included in the resulting models. For a more accurately constrained stochastic DFN model, constraints should be applied with the highest degree of precision available with respect to the time budgeted for parameterizing the model.

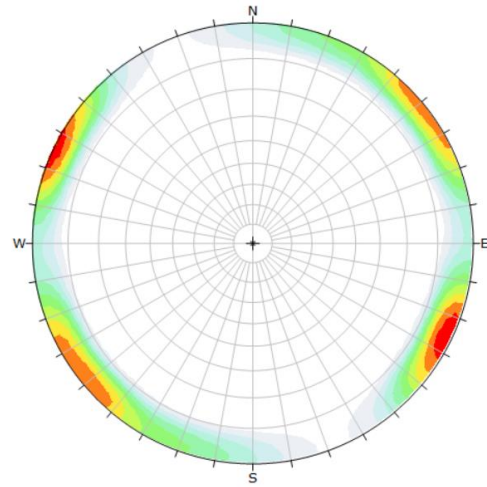


Fig. 13. Wulff stereonet representing fractures of DFN model generated with parameters derived from additional preprocessing

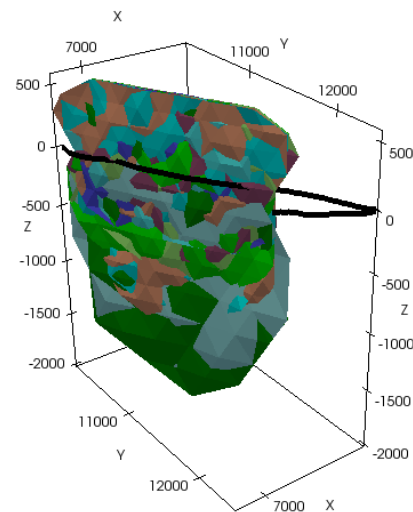


Fig. 14. Input trace for fracture 8 and the resulting fractures from ten separate DFN realizations of the deterministic data.

ACKNOWLEDGEMENTS

Nuclear Waste Management Organization (NWMO) support of the MoFrac project is greatly appreciated, and in particular, Eric Sykes provided insightful feedback.

REFERENCES

1. Anderson, D.L., Ames, D.P. and Yang, P. 2014. Quantitative methods for comparing different polyline stream network models. *Journal of Geographic Information Systems*. (6)
2. Bonnet, E., Bour, O., Odling, N.E., Davy, P., Main, I., Cowie, P. and Berkowitz, B. 2001. Scaling of fracture systems in geological media. *Reviews of Geophysics* (39) 3.
3. Gierszewski, P., Avis, J., Calder, N., D'Andrea, A., Garisto, F., Kitson, C., Melnyk, T. and Wojciechowski, L. 2004. *Third Case Study - Postclosure Safety Assessment Deep Geological Repository Technology Program Report No: 06819-REP-01200-10109-R00*, Ontario Power Generation, Toronto, Ontario.
4. Junkin, W., Janeczek, D., Bastola, S., Wang, X., Cai, M., Fava, L., Sykes, E., Munier, R., and Srivastava, R.M. 2017. Discrete Fracture Network Generation for the Äspö TAS08 Tunnel using MoFrac. *ARMA 2017, The 51st US Rock Mechanics/Geomechanics Symposium, San Francisco, California, 2017*.
5. Neuman, S.P. 2008. Multiscale relationship between fracture length aperture, density, and permeability. *Geophysical Research Letters* (35).
6. Niven, E.B. and Deutsch, C.D. 2010. Relating different measures of fracture intensity. Paper 103, *CCG Annual Report 12*.
7. Rocscience. 2015. DIPS. Ver. 6.0.17.
8. Srivastava, R.M. 2002. *The discrete fracture network model in the local-scale flow system for the third case study*. Deep Geological Repository Technology Program Report 06819-01300-10061, Ontario Power Generation, Toronto, Ontario.
9. Srivastava, R.M. 2006. Field Verification of a geostatistical method for simulating fracture network models. Golden Rocks 2006, *The 41st Symposium on Rock Mechanics (USRMS), Golden, Colorado, 2006*.